ChemComm

COMMUNICATION

View Article Online
View Journal | View Issue

Cite this: *Chem. Commun.*, 2015, 51, 8849

Received 13th March 2015,
Accepted 16th April 2015

DOI: 10.1039/c5cc02138c

www.rsc.org/chemcomm

Effect of ionic interaction on the mechanochromic properties of pyridinium modified tetraphenylethene†

Ting Hu,[a] Bicheng Yao,[a] Xiujuan Chen,[a] Weizhang Li,[b] Zhegang Song,[c] Anjun Qin,[b] Jing Zhi Sun*[a] and Ben Zhong Tang*[abc]

A pyridinium modified tetraphenylethene-based salt shows aggregation-induced emission enhancement properties and irreversible mechanochromic behaviours.

As typical soft materials, molecular solids tend to show more pronounced responses to external stimuli when compared to covalent and ionic solids. For conjugated organic compounds, the responses reflect not only the macroscopic change in shape and the microscopic change in molecular packing, but also the optic and electronic properties. A representative example is the mechano-chromic effect observed for many organic dyes that possess aggregation-induced emission (AIE) or aggregation-induced emission enhancement (AIEE) properties.[1,2] The term mechano-chromism refers to the phenomenon in which a solid changes its absorption and/or emission spectrum under a certain kind of mechanical force applied to it.[1a,3] For organic AIE/AIEE solids, the incentives are largely classified into two categories. One is the change of physical factors and the other is rooted in the chemical structures.

The physical factors that result in mechanochromism can be further divided into intramolecular and intermolecular changes, which are conformation (*e.g.* torsional angle) and molecular packing (*e.g.* J-aggregate), respectively. Regardless of the formation and fracture of a chemical bond, the potential barrier of the mechano-chromism induced by physical factors is relatively low and the process is usually reversible. For instance, most of the AIE/AIEE materials show higher emission efficiency in the crystal state but the efficiency becomes lower, accompanied by a red-shifted emission spectrum, when crystals are transformed into amorphous solids by mechanical forces such as grounding and shearing. These feature changes can be fully recovered by appropriate thermal annealing and/or vapor fuming.[1a,4] This allows organic AIE/AIEE solids to be used as smart action elements such as mechano-sensors, security papers, and data storage devices. To this end, the softness and reversibility are highly desirable. But the evident reversibility and softness make such kind of organic solids not stable enough to sustain long term storage or to endure stronger external stress. In fact, the amorphous state of organic solids is metastable and it is destined to enter the most stable crystal state under appropriate conditions or in a period that is long enough. Therefore, it is a challenging task to postpone the spontaneous transition from amorphous to crystal states.

Static attraction between cationic and anionic species is stronger than the van der Waals interaction between uncharged species. As the two opposite poles, most inorganic salts show high hardness and melting points, while some organic salts can be ionic liquids at room temperature. These features suggest that, with rationally designed size and symmetry, the ionic compounds constructed using large organic cations and small inorganic anions are expected to keep the balance between the rigidity of an ionic solid and the flexibility of a covalent solid.

The strategy of taking advantage of ionic interaction to enhance the emission of organic luminogens has been reported by F. Fery-Forgues and colleagues. 4-Hydroxy-7-nitrobenzoxadiazole phenolate anions and tetrabutylammonium bromide cations formed a hydrophobic salt, which readily crystallized in the medium and was accompanied by a strong increase in fluorescence intensity.[5] Lately, this strategy was carried forward and expanded by different research groups in fluorescence turn-on detection of ionic chemicals and charged biomacromolecules, such as heparin and DNA.[6–8]

Recently, we reported an ion pair containing tetraphenylethene (TPE) derivative, $[TPE\text{-}Py\text{-}Me]^+[PF_6]^-$ (Chart S1, ESI†).[9,10]

[a] *MoE Key Laboratory of Macromolecular Synthesis & Functionalization, Department of Polymer Science and Engineering, Zhejiang University, Hangzhou 310027, China. E-mail: sunjz@zju.edu.cn*

[b] *Guangdong Innovative Research Team, State Key Laboratory of Luminescent Materials and Devices, South China University of Technology, Guangzhou 510640, China*

[c] *Department of Chemistry, Institute for Advanced Study, Institute of Molecular Functional Materials, and State Key Laboratory of Molecular Neuroscience, The Hong Kong University of Science & Technology, Clear Water Bay, Kowloon, Hong Kong, China. E-mail: tangbenz@ust.hk*

† Electronic supplementary information (ESI) available: Synthesis and characterization, materials, procedures for all experiments; additional absorption/emission spectra; photographs of fluorescence emission; TGA and DSC curves. See DOI: 10.1039/c5cc02138c

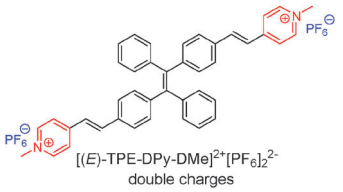

Chart 1 Molecular structures of $[(E)\text{-TPE-DPy-DMe}]^{2+}[PF_6]_2^{2-}$.

It is a typical AIEE molecule and showed evident mechanochromic effects. Like other uncharged TPE-derivatives, the solid-state emission of $[\text{TPE-Py-Me}]^{+}[PF_6]^{-}$ was reversibly switched between green and yellow colors by grinding–fuming and grinding–heating processes with a high contrast due to the transformation from the crystalline to the amorphous state and *vice versa*. Despite the similarity, the chromic switching occurred with greater difficulty than for those uncharged TPE-derivatives. For example, the emission of the ground powder of $[\text{TPE-Py-Me}]^{+}[PF_6]^{-}$ was recovered by fuming with acetone vapor for 10 min or heating at 150 °C for 10 min. Another charge-free TPE derivative BPHTATPE displayed excellently reversible mechano-chromic behaviours (Chart S1, ESI†). The heating of the ground or pressurized sample at 120 °C for a short while (1 min) or the fuming of the ground sample with the vapor of polar solvents for 3 min could recover its emission color, although BPHTATPE has a larger molecular weight than $[\text{TPE-Py-Me}]^{+}[PF_6]^{-}$.[11] Based on these comparative results, we realize that the introduction of ionic interaction is helpful to acquire more robust mechanochromic effects and non-volatile emission colour changes.

Herein, we report our attempt to enhance the robustness of the mechanochromism by introducing more ionic species into an AIE-active molecule. As shown in Chart 1, it is a homolog of $[\text{TPE-Py-Me}]^{+}[PF_6]^{-}$, in which the AIE-gen, cationic and anionic moieties are TPE, pyridinium and hexafluorophosphate ($[PF_6]^{-}$), respectively. This compound ($[\text{TPE-DPy-DMe}]^{2+}[PF_6]_2^{2-}$) demonstrates typical AIEE and mechanochromic behaviors as most TPE derivatives have shown. But the experimental data reveal that the transition between the highly efficient yellow emission of the crystalline and the moderate red emission of the amorphous $[\text{TPE-DPy-DMe}]^{2+}[PF_6]_2^{2-}$ solid becomes irreversible by simple treatments of thermal annealing and/or solvent vapor fuming, whereas the ground sample can recover its emission only by recrystallization from dissolving the amorphous solid in suitable solvents. These behaviours are evidently distinct from the phenomena observed for $[\text{TPE-Py-Me}]^{+}[PF_6]^{-}$ and other uncharged TPE derivatives.

The synthetic route towards $[\text{TPE-DPy-DMe}]^{2+}[PF_6]_2^{2-}$, the experimental procedures and the structure characterization data are described in the ESI† (Schemes S1, S2 and Fig. S1–S9). In brief, the dibromo-modified TPE was derived from a McMurry coupling reaction and the resultant was a mixture of *E*/*Z* isomers. The mixture was directly used in the successive Heck reaction, through which the pyridine moieties were linked to the TPE core *via* C=C double bonds. The Heck reaction allowed both of the C=C bridges to be in sole *trans*-configuration, which has been confirmed by the characteristic chemical shifts and coupling constant in the ^{1}H NMR spectrum (Fig. S1, ESI†). The *E* and *Z* isomers of the pyridine-modified TPE (TPE-DPy) could be readily separated by using silicon gel column chromatography with the mixture of petroleum (60–90 °C) and tetrahydrofuran (5 : 1 by volume) as the eluent, and the *E*-isomer was the predominant resultant in a total yield of 37%. Then, the pure *E*-isomer of TPE-DPy was used to react with iodomethane at room temperature to give rise to $[\text{TPE-DPy-DMe}]^{2+}[I]_2^{2-}$, which is an organic salt. This salt emits yellow fluorescence in the crystalline state and has a relatively low quantum efficiency (Φ = 0.8%), due to the presence of iodine anions, which partially quenched the fluorescence. Therefore, we replaced the iodine anions by $[PF_6]^{-}$ anions and got the target compound $[\text{TPE-DPy-DMe}]^{2+}[PF_6]_2^{2-}$ in a good yield of 96%. The as-prepared crystalline powder of $[\text{TPE-DPy-DMe}]^{2+}[PF_6]_2^{2-}$ emits strong yellow-greenish fluorescence with an emission peak (λ_{em}) at 558 nm and an evidently enhanced quantum efficiency (Φ) of 43% (Fig. S10, ESI†). The characterization data indicate that the $[\text{TPE-DPy-DMe}]^{2+}[PF_6]_2^{2-}$ molecule takes a *trans*-configuration and the following experimental results are based on this *E*-isomer $[(E)\text{-TPE-DPy-DMe}]^{2+}[PF_6]_2^{2-}$.

$[(E)\text{-TPE-DPy-DMe}]^{2+}[PF_6]_2^{2-}$ is soluble in acetone but insoluble in hexane. Thus we used acetone and hexane as solvent and non-solvent to examine the AIE behaviours of the salt and the results are shown in Fig. 1. In dilute acetone solution (1×10^{-5} mol L^{-1}), it shows a faint emission when excited at a wavelength of 395 nm (λ_{ex}, the maximum of the salt's UV-vis absorption spectrum, see Fig. S11, ESI†). It remains weakly emissive in the acetone–hexane mixtures with increasing the hexane fraction (f_H, by volume) to 60%, and λ_{em} appears at around 600 nm. When the f_H is up to 70%, the mixture becomes evidently emissive and λ_{em} blue-shifts to about 586 nm. Further increasing the f_H to 80% and 90%, the emission intensity grows higher and λ_{em} localizes at around 586 nm. The f_H dependent fluorescence behavior is displayed in Fig. 1B, which indicates that the salt is a typical AIEE-active molecule.

The blue-shifted fluorescence spectrum can be ascribed to the solvatochromic effect of the $[(E)\text{-TPE-DPy-DMe}]^{2+}[PF_6]_2^{2-}$ molecule. This effect usually occurs in fluorogens bearing

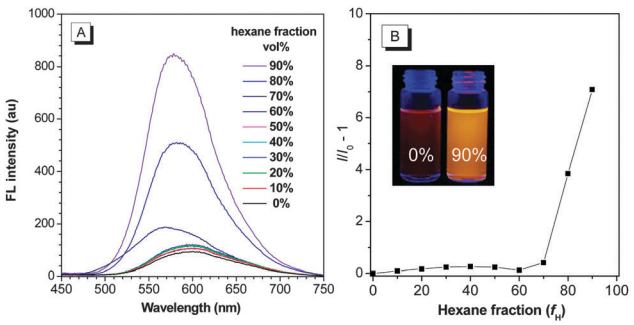

Fig. 1 (A) Fluorescence (FL) spectra of $[(E)\text{-TPE-DPy-DMe}]^{2+}[PF_6]_2^{2-}$ in acetone–hexane mixtures with different hexane fractions (f_H). (B) Plot of the f_H-dependent peak FL intensity, where I_0 and I are the peak FL intensities at f_H = 0 and other fractions, respectively; and the data are extracted from (A). $[(E)\text{-TPE-DPy-DMe}]^{2+}[PF_6]_2^{2-}$ concentration: 10^{-5} M. Excitation wavelength (λ_{ex}): 395 nm. Inset of (B): FL images of $[(E)\text{-TPE-DPy-DMe}]^{2+}[PF_6]_2^{2-}$ in acetone–hexane mixtures taken at f_H = 0% and f_H = 90%. λ_{ex}: 365 nm.

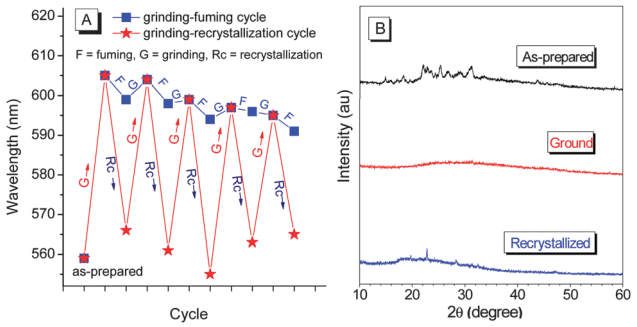

Fig. 2 (A) Variations of the emission wavelengths of $[(E)\text{-TPE-DPy-DMe}]^{2+}[PF_6]_2^{2-}$ solids in grinding–fuming (blue trace) and grinding–recrystallization (red trace) cycles. (B) X-ray diffraction patterns for $[(E)\text{-TPE-DPy-DMe}]^{2+}[PF_6]_2^{2-}$ of as-prepared microcrystal (upper), ground powder (middle) and re-crystalline samples (lower).

electron donor (D) and acceptor (A) moieties.[12] Such fluorogens usually show a red-shifted fluorescence spectrum and concomitantly decreased fluorescence intensity as the polarity of the environment enhances. In a $[(E)\text{-TPE-DPy-DMe}]^{2+}[PF_6]_2^{2-}$ molecule, the TPE core and the pyridinium units play the roles of D and A, respectively. Thus it should have a typical solvatochromic behaviour. Indeed, this behaviour has been confirmed by monitoring the absorption and emission spectra of $[(E)\text{-TPE-DPy-DMe}]^{2+}[PF_6]_2^{2-}$ in a series of organic solvents with different polarities. As displayed in Fig. S12 (ESI†), the emission maximum shifts from 565 to 613 nm when the solvent changes from non-polar dioxane to highly polar ethanol.

A lumpy solid was obtained after the solvents were fully evaporated, and it was used to investigate the mechanochromic behaviours. The as-synthesized $[(E)\text{-TPE-DPy-DMe}]^{2+}[PF_6]^{2-}$ is a light yellow solid with a strong yellow-greenish emission peak at ~560 nm (Fig. 2A). After the lumpy solid was ground into a fine powder with a pestle or shearing with a spatula, the emission peak shifts to around 605 nm, showing a red-shift of 45 nm. The emission peak exhibits a trend of a monotonous blue-shift in grinding–fuming cycles. This phenomenon can be associated with the accumulation of the fuming effect.[13] The fluorescence intensity of the ground $[(E)\text{-TPE-DPy-DMe}]^{2+}[PF_6]_2^{2-}$ powder is much weaker than that of the untreated sample (ref the images in Fig. 3). Quantitatively, the quantum efficiency drops from 43% to 18% by grinding treatment. This is a typical mechanochromic behaviour that has been observed for a variety of AIE/AIEE compounds.[1–3] The change of emission colour is associated with the changes of the molecular packing in the solids before and after grinding. X-ray diffraction patterns of $[(E)\text{-TPE-DPy-DMe}]^{2+}[PF_6]_2^{2-}$ samples indicate that the as-prepared and ground solids are in polycrystalline and amorphous states, respectively (Fig. 2B).

It has been found that a variety of uncharged TPE-based molecules exhibit a solvent-dependent vapochromic effect.[2–6] Their ground samples are sensitive to volatile polar solvents. After exposure to the solvent vapor for a while, the red-shifted emission of the ground samples is largely reverted back to the original emission of the as-prepared sample, owing to the fuming-induced recrystallization process. We investigated the vapochromic effect of $[(E)\text{-TPE-DPy-DMe}]^{2+}[PF_6]_2^{2-}$ by exposure of the ground sample to the dichloromethane (DCM) vapor for ~5 min. But the emission had not been recovered to the original yellow-greenish. Using the first cycle as an example, the grinding resulted in a red-shift of the emission peak from 558 to 605 nm. The DCM vapor fuming for 5 min could only lead to a blue-shift of the emission peak from 605 to 598 nm. Extending the fuming time to 10 min brought about little change in the emission features. However, when the amorphous ground powder was redissolved in DCM and dried, the emission intensity and colour reversed almost to the solid before grinding. In the first cycle, the emission peak shifted from 605 to 565 nm. The XRD pattern recorded from the recrystallization sample (Fig. 2B) indicated a crystalline state that is similar to the as-prepared solid.

According to the thermodynamic principles, the amorphous ground sample is in a metastable state, thus it will transform back to the thermo-dynamically stable crystalline state. This transformation can be achieved by thermal annealing. To fix the annealing temperature, the thermal transition properties were evaluated by taking thermal gravimetric analysis (TGA) and differential scanning colorimetry (DSC) measurements at a scan rate of 10 °C min^{-1} under a nitrogen flow (Fig. S13 and S14, ESI†). The decomposition temperature of the $[(E)\text{-TPE-DPy-DMe}]^{2+}[PF_6]_2^{2-}$ powder is determined to be 340 °C. The as-prepared crystalline solid shows an endo-thermal transition peak at 265 °C and is immediately followed by an exo-thermal transition peak at around 274 °C. The first peak can be assigned to the melting point of the microcrystals and the second may be associated with the recrystallization of the melt just formed. After grinding, the fine powder only has an exo-thermal transition at around 263 °C, which is tentatively assigned to the amorphous to crystal transition. The sample recrystallized from the ground powder in DCM shows a thermal transition behaviour similar to the as-prepared microcrystals, having an endo-thermal transition peak at 252.7 °C and immediately follows an exo-thermal transition peak at 268.5 °C. The small decrease in the melting point can be explained by the fact that the recrystallized sample has a relatively low degree of crystallization, which is in accordance with what is revealed by XRD patterns (Fig. 2B).

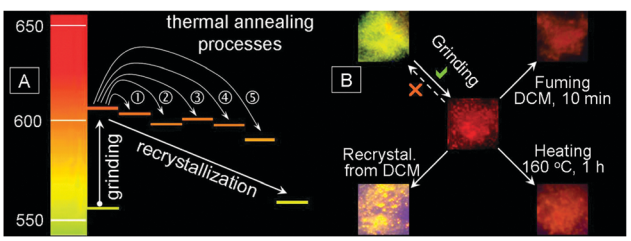

Fig. 3 (A) Emission peak (colour) changes of $[(E)\text{-TPE-DPy-DMe}]^{2+}[PF_6]_2^{2-}$ samples upon grinding the as-prepared microcrystals, heating the ground powders at different temperatures (① 120 °C, 1 h; ② 140 °C, 1 h; ③ 160 °C, 1 h; ④ 180 °C, 1 h; ⑤ 180 °C, 2 h) and the recrystallization of the ground powders in the DCM solution. (B) Photographs of the light emission (λ_{ex} = 365 nm) from the samples of as-prepared crystalline, ground powders, DCM vapor fuming, thermal annealing, and recrystallization from DCM.

Based on the thermal evaluation results, we investigated the effect of thermal annealing on the mechanochromic behaviours of the ground $[(E)\text{-TPE-DPy-DMe}]^{2+}[PF_6]_2^{2-}$ sample. As shown in Fig. 3, the emission peak undergoes a blue-shift of about only 2 nm after annealing at 120 °C for 1 h. In a typical run of elevating the annealing temperature to 140, 160 and 180 °C and setting an annealing time of 1 h, the blue-shifts of the emission peak are recorded as 6, 3, and 6 nm, respectively. Extending the thermal annealing at 180 °C to 2 h, the emission peak shift is about 12 nm. The larger spectral shift at higher temperature and for longer time is reasonable because of the metastable state of the ground sample. All of these spectral shifts are quite small if compared with that observed for the spectral shift between the ground and the recrystallized samples (>40 nm).[1]

The above experimental results indicate that the mechanochromic behaviour of $[(E)\text{-TPE-DPy-DMe}]^{2+}[PF_6]_2^{2-}$ is irreversible by simple solvent vapor fuming and thermal annealing treatments. But the emission features can only be reverted from the mechanically treated (ground) sample to the original (as-prepared) one by recrystallization treatments. This behaviour is evidently distinct from the reversible mechanochromism observed for many uncharged TPE-based molecules reported in the recent literature. Considering that the basic difference between the previously reported molecules and the present $[(E)\text{-TPE-DPy-DMe}]^{2+}[PF_6]_2^{2-}$ focuses on the existence or absence of the sufficient static charges in molecules, we ascribe the lowered reversibility and enhanced robust mechanochromic effects of $[(E)\text{-TPE-DPy-DMe}]^{2+}[PF_6]_2^{2-}$ to the static interaction between the charged species. On the one hand, the static interaction has no directionality and saturability, thus each of the negatively charged $[PF_6]^-$ is an attractive center to surrounding positively charged $[(E)\text{-TPE-DPy-DMe}]^{2+}$ species and *vice versa*. The ionic interaction between net charges, on the other hand, is stronger than the van der Waals interaction. In addition, the unmatched sizes between the positively and negatively charged species make the amorphous solid more stable, as demonstrated by ionic liquids. Consequently, the amorphous ground sample of $[(E)\text{-TPE-DPy-DMe}]^{2+}[PF_6]_2^{2-}$ exhibits extraordinary stability.

In summary, we have shown that the modification of TPE fluorogens with ionic groups allows the derived TPE-based salt to exhibit AIEE activity and to achieve effectively enhanced mechanochromic robustness (Fig. S15, ESI†). With only weak van der Waals interaction, the molecular solid of the TPE-derivative exhibits highly reversible mechanochromic behaviours at a moderate thermal annealing temperature and shorter solvent vapor fuming time. Introducing an ionic species into the TPE-derivative, $[\text{TPE-Py-Me}]^+[PF_6]^-$ exhibits reversible mechano-chromic behaviours at elevated annealing temperature and longer fuming time. Enhancement of the ionic strength, $[\text{TPE-DPy-DMe}]^{2+}[PF_6]_2^{2-}$ exhibits irreversible mechanochromic behaviours at elevated annealing temperature and longer fuming time. The emission features can only be reverted from the mechanically treated (ground) sample to the original (as-prepared) one by recrystallization treatment. The distinct behaviours are reasonably ascribed to the static interaction between the cationic and anionic species, which bestows the solid with excessive stability in comparison with uncharged TPE-derivatives. The present work gives a hint to rationally design organic photo/electronic materials and to acquire an ingenious balance between the robustness of ionic solids and the flexibility of covalent solids.

This work was financially supported by the key project of the Ministry of Science and Technology of China (2013CB834704), the National Science Foundation of China (51273175), the Research Grants Council of Hong Kong (16301614, N_HKUST604/14 and N_HKUST620/11) and the Guangdong Innovative Research Team Program (201101C0105067115).

Notes and references

1 (*a*) J. Mei, Y. Hong, J. W. Y. Lam, A. Qin, Y. Tang and B. Z. Tang, *Adv. Mater.*, 2014, **26**, 5429; (*b*) Z. Chi, X. Zhang, B. Xu, X. Zhou, C. Ma, Y. Zhang and J. Xu, *Chem. Soc. Rev.*, 2012, **41**, 3878; (*c*) Y. Hong, J. W. Y. Lam and B. Z. Tang, *Chem. Soc. Rev.*, 2011, **40**, 5361.

2 (*a*) E. P. J. Parrott, N. Y. Tan, R. Hu, A. Zeitler, B. Z. Tang and E. Pickwell-MacPherson, *Mater. Horiz.*, 2014, **1**, 251; (*b*) Z. Zhao, C. Y. K. Chan, S. Chen, C. Deng, J. W. Y. Lam, C. K. W. Jim, Y. Hong, P. Lu, Z. Chang, X. Chen, H. S. Kwok, H. Qiu and B. Z. Tang, *J. Mater. Chem.*, 2012, **22**, 4527; (*c*) C. Weder, *J. Mater. Chem.*, 2011, **21**, 8235; (*d*) G. Q. Zhang, J. W. Lu, M. Sabat and C. L. Fraser, *J. Am. Chem. Soc.*, 2010, **132**, 2160; (*e*) Y. Dong, J. W. Y. Lam, A. Qin, J. Sun, J. Liu, Z. Li, J. Sun, H. H. Y. Sung, I. D. Williams, H. S. Kwok and B. Z. Tang, *Chem. Commun.*, 2007, 3255.

3 (*a*) K. Ariga, T. Mori and J. P. Hill, *Adv. Mater.*, 2012, **24**, 158; (*b*) A. Pucci and G. Ruggeri, *J. Mater. Chem.*, 2011, **21**, 8282; (*c*) Y. Sagara and T. Kato, *Nat. Chem.*, 2009, **1**, 605.

4 (*a*) Y. Dong, B. Xu, J. Zhang, X. Tan, L. Wang, J. Chen, H. Lv, S. Wen, B. Li, L. Ye, B. Zou and W. Tian, *Angew. Chem., Int. Ed.*, 2012, **51**, 10782; (*b*) Z. Zhang, B. Xu, J. Su, L. Shen, Y. Xie and H. Tian, *Angew. Chem., Int. Ed.*, 2011, **50**, 11654; (*c*) S.-J. Yoon and S. Park, *J. Mater. Chem.*, 2011, **21**, 8338; (*d*) X. Lou, J. Li, C. Li, L. Heng, Y. Q. Dong, Z. Liu, Z. Bo and B. Z. Tang, *Adv. Mater.*, 2011, **23**, 3261.

5 (*a*) J. Chahine, N. Saffon, M. Cantuel and S. Fery-Forgues, *Langmuir*, 2011, **27**, 2844; (*b*) J.-F. Lamere, N. Saffon, I. Dos Santos and S. Fery-Forgues, *Langmuir*, 2010, **26**, 10210; (*c*) C. Yi, C. Blum, S.-X. Liu, Y.-F. Ran, G. Frei, A. Neels, H. Stoeckli-Evans, G. Calzaferri, S. Leutwyler and S. Decurtins, *Cryst. Growth Des.*, 2008, **8**, 3004.

6 (*a*) Y. Dong, J. W. Y. Lam, A. Qin, J. Liu, Z. Li and B. Z. Tang, *Appl. Phys. Lett.*, 2007, **91**, 011111; (*b*) Q. Zhao, S. Zhang, Y. Liu, J. Mei, S. Chen, P. Lu, A. Qin, Y. Ma, J. Z. Sun and B. Z. Tang, *J. Mater. Chem.*, 2012, **22**, 7387; (*c*) Y. Lin, G. Chen, L. Zhao, W. Z. Yuan, Y. M. Zhang and B. Z. Tang, *J. Mater. Chem.*, 2015, **3**, 112.

7 (*a*) Y. Liu, A. Qin, X. J. Chen, X. Y. Shen, L. Tong, R. Hu, J. Z. Sun and B. Z. Tang, *Chem. – Eur. J.*, 2011, **17**, 14736; (*b*) N. B. Shustova, T. C. Ong, A. F. Cozzolino, V. K. Michaelis, R. G. Griffin and M. Dinca, *J. Am. Chem. Soc.*, 2012, **134**, 10561; (*c*) N. B. Shustova, A. F. Cozzolino, S. Reineke, M. Baldo and M. Dincă, *J. Am. Chem. Soc.*, 2013, **135**, 13326; (*d*) P. Verwilst, K. Sunwoo and J. S. Kim, *Chem. Commun.*, 2015, **51**, 5556.

8 (*a*) X. Yan, D. Xu, X. Chi, J. Chen, S. Dong, X. Dong, Y. Yu and F. Huang, *Adv. Mater.*, 2012, **24**, 362; (*b*) S. Dong, B. Zheng, D. Xu, X. Yan, M. Zhang and F. Huang, *Adv. Mater.*, 2012, **24**, 3191; (*c*) W. Bai, Z. Wang, J. Tong, J. Mei, A. Qin, J. Z. Sun and B. Z. Tang, *Chem. Commun.*, 2015, **51**, 1089.

9 Z. Na, M. Li, Y. Yan, J. W. Y. Lam, Y. L. Zhang, Y. S. Zhao, K. S. Wong and B. Z. Tang, *J. Mater. Chem. C*, 2013, **1**, 4640.

10 F. Anariba, L. L. Chng, N. S. Abdullah and F. E. H. Tayx, *J. Mater. Chem.*, 2012, **22**, 19303.

11 J. Wang, J. Mei, R. Hu, J. Z. Sun, A. Qin and B. Z. Tang, *J. Am. Chem. Soc.*, 2012, **134**, 9956.

12 (*a*) E. Lippert, *Z. Naturforsch., A: Phys. Sci.*, 1955, **10**, 541; (*b*) C. Reichardt, *Chem. Rev.*, 1994, **94**, 2319.

13 (*a*) R. Misra, T. Jadhav, B. Dhokale and S. M. Mobin, *Chem. Commun.*, 2014, **50**, 9076; (*b*) P. Gautam, R. Maragani, S. M. Mobin and R. Misra, *RSC Adv.*, 2014, **4**, 52526; (*c*) T. Jadhav, B. Dhokale, S. M. Mobin and R. Misra, *RSC Adv.*, 2015, **5**, 29878.

